HHS Public Access

Author manuscript

J Immunol. Author manuscript; available in PMC 2021 August 01.

Published in final edited form as:

J Immunol. 2020 August 01; 205(3): 801–810. doi:10.4049/jimmunol.2000186.

Human Natural Killer Cell Cytoskeletal Dynamics and Cytotoxicity are Regulated by LIM Kinase

Melody G. Duvall[1,2], **Mary E. Fuhlbrigge**[1], **Roisin B. Reilly**[1], **Katherine H. Walker**[1], **Ayşe Kılıç**[1,3], **Bruce D. Levy**[1,*]

[1]Division of Pulmonary and Critical Care Medicine, Department of Medicine, Brigham and Women's Hospital, Harvard Medical School, Boston, MA 02115, USA

[2]Division of Critical Care Medicine, Department of Anesthesiology, Critical Care and Pain Medicine, Boston Children's Hospital, Harvard Medical School, Boston, MA 02115, USA

[3]Channing Division of Network Medicine, Department of Medicine, Brigham and Women's Hospital, Harvard Medical School, Boston, MA 02115, USA

Abstract

Natural killer (NK) cells provide immune surveillance and host protection against viruses and tumors through their cytotoxic effector function. Cytoskeletal rearrangement is necessary for NK cell lytic granule trafficking and immune synapse formation to trigger apoptosis of targeted cells. LIM kinase (LIMK) regulates F-actin remodeling by phosphorylating cofilin to inhibit actin severing and depolymerization. Here, in human NK cells, the glucocorticoid dexamethasone down-regulated LIMK expression, F-actin accumulation at the immune synapse, lytic granule trafficking, and cytotoxicity. In contrast, the specialized pro-resolving mediator lipoxin A_4 (LXA_4) promoted NK cell LIMK expression, lytic granule polarization to the immune synapse and cytotoxicity. Using a LIMK inhibitor, we show that LIMK activity is necessary for NK cell cytotoxicity, including LXA_4's pro-resolving actions. Together, our findings identify LIMK as an important control mechanism for NK cell cytoskeletal rearrangement that is differentially regulated by glucocorticoids and specialized pro-resolving mediators to influence NK cell cytotoxicity.

Introduction

Natural killer (NK) cells are innate lymphocytes important for host defense against viruses and tumors (1, 2). NK cell cytotoxicity requires formation of an immune synapse and directed delivery of lytic granules that activate apoptosis in targeted cells (3). NK cell lytic granule mobilization proceeds via cytoskeletal rearrangement to facilitate lytic granule

*Corresponding Author: Bruce D. Levy, 60 Fenwood Road, Boston, MA, 02115, USA. Phone: 617-525-5407; Fax: 617-732-7421; blevy@bwh.harvard.edu.

Author Contributions: MGD, MEF, and RBR designed the study, performed experiments, collected and analyzed data, and wrote the manuscript. KHW and AK analyzed the data and wrote the manuscript. BDL conceived the study, designed experiments, analyzed data, and wrote the manuscript.

Data and Materials Availability: The data supporting the results in this study are available within the paper and in its Supplementary Information.

trafficking to the microtubule organizing center (MTOC), polarization of the MTOC to the immune synapse, and polymerization of F-actin at the mature synapse to anchor NK cell degranulation into the target cell (4). Genetic mutations in actin-regulating cytoskeletal proteins including WASp, DOCK8, and Coronin1A have been associated with abnormal actin remodeling and impaired NK cell cytotoxicity (5–7).

In addition to host defense, NK cells are effectors for resolution of inflammation by promoting apoptosis of granulocytes and lymphocytes for clearance from inflamed tissues (8, 9). The resolution of acute inflammation is an active process promoted in part by endogenous specialized pro-resolving mediators (SPMs) that signal to halt inflammation and promote tissue catabasis (10, 11). Human NK cells express receptors for several families of SPMs, including the lipoxin A_4 (LXA_4) high affinity receptor ALX/FPR2 (9, 12). NK cells respond to LXA_4, which enhances NK cell resolution effector functions (9, 12). Patients with severe asthma have chronic “unresolved” inflammation with defective SPM production (13) and impaired NK cell cytotoxicity (12). Of note, severe asthma patients are prescribed high doses of corticosteroids, which are often ineffective in controlling airway inflammation in these patients and can further diminish NK cell function (12, 14, 15). More information is needed to understand molecular mechanisms that control NK cell function and how exogenous exposures can influence these protective and pro-resolving innate lymphocytes.

Here, we identified LIM kinase (LIMK) as a pivotal effector of NK cell cytoskeletal rearrangement and cytotoxicity that is inhibited by the glucocorticoid dexamethasone and induced by the SPM LXA_4. Inhibition of LIMK disrupted F-actin accumulation at the NK cell immune synapse, prevented MTOC polarization and lytic granule delivery to the target cell, and impaired cytotoxicity. These findings support an important role for LIMKs as cytoskeletal regulators of NK cell cytotoxicity that are downstream of endogenous immunomodulatory signals (*i.e.* LXA_4).

Materials and Methods

NK cell isolation and culture

Healthy human leukopaks were obtained as discarded materials from de-identified blood donors from the Boston Children’s Hospital Blood Donor Center. PBMC were isolated by density centrifugation over Histopaque-1077 (Sigma). NK cells were enriched by negative selection (EasySep human NK cell enrichment kit; StemCell Technologies). Purity of NK cells was ≥ 95% $CD3^{-}CD56^{+}$. NK cells were cultured in RPMI 1640 (Sigma) with 1 ng/mL IL-15 (Invitrogen), 2% human serum (Sigma), 2 mM L-glutamine, 1 mM sodium pyruvate, 25 mM HEPES, non-essential amino acids, penicillin (100 IU/mL) and streptomycin (100 μg/mL). NK cells were exposed to vehicle (0.1% ethanol), dexamethasone (1 μM; Sigma), or LXA_4 (100 nM; Cayman Chemical) for 48 hours and re-dosed at 24 hours. For concentration response experiments, NK cells were exposed to four to five-log increasing concentrations of dexamethasone (100 pM to 1 μM) or LXA_4 (100 pM to 100 nM). These concentrations were chosen based on prior published literature evaluating the effect of dexamethasone or other corticosteroids on human NK cells (14, 16–19) and LXA_4 or other SPMs on human NK cells, monocytes, or PBMC (9, 12, 20–24).

NK cell cytotoxicity assay

NK cells exposed to noted conditions for 48 hours were subsequently co-incubated with K562 target cells labeled with 5 μM CellTrace Violet (Invitrogen) at an effector:target ratio of 5:1 for 4 hours at 37°C in 5% CO_2. NK cell-mediated target cell apoptosis was assessed by flow cytometry staining for Annexin V and 7-AAD on CellTrace Violet expressing K562 target cells.

Flow cytometry

The following antibodies specific for human proteins were used, with clones noted in parentheses: anti-CD3 PerCP (UCHT1), anti-NKp46 APC (9E2), anti-NKG2D FITC (1D11), and anti-CD56 PE-Cy7 (HCD56) all from Biolegend. NK cells were collected after 48 hours of exposure to noted conditions and incubated with Fc receptor blocking solution (Human TruStain FcX, Biolegend) for 10 minutes at 4°C before specific surface staining for 20 minutes at 4°C. Cells were then washed and fixed with 2% paraformaldehyde. Data were acquired on an LSR Fortessa flow cytometer (BD Biosciences) and analyzed using FlowJo software version 10.1 (TreeStar). NK cells were identified as cells with lymphocyte morphology by forward scatter and side scatter that lacked CD3 expression and expressed CD56.

Immunofluorescence microscopy

NK cells exposed to vehicle, dexamethasone, or LXA_4 for 48 hours were co-incubated with target K562 cells at 1:2 ratio for 2 hours at 37°C in 5% CO_2. Poly-L-lysine coated slides were coated with anti-CD58 antibody for target cell immobilization. NK:target co-cultures were adhered to slides for 30 minutes at 37°C, fixed with 4% paraformaldehyde, permeabilized with 0.2% Triton X100, blocked with 5% goat serum (Sigma) and stained with AlexaFluor488-conjugated anti-perforin (dG9; BioLegend) for 45 minutes at 37°C. Slides were mounted with 0.15 mm coverslips using ProLong Gold with DAPI (Invitrogen). Images were acquired in a single z-plane using a Zeiss immunofluorescence microscope with 40X objective. The mean area-weighted distance of lytic granules from the target cell immune synapse was calculated using immunofluorescence images, as follows (Supplemental Fig. 1).

Calculation of lytic granule distance from immune synapse

NK:target conjugates were identified by light and the perimeters were outlined as regions of interest (ROI) in ImageJ (Supplemental Fig. 1). The immune synapse was defined as the overlapping area of the NK cell and target cell ROIs and the X and Y coordinates of each endpoint of the immune synapse were noted. Individual NK cell lytic granules were identified as discrete objects with positive fluorescence intensity in the FITC channel (perforin) above background threshold and the centroid X and Y coordinates and area of each granule were noted as in (25). An average of 4 lytic granule regions were observed per NK cell (range 1–9). The distance of each individual lytic granule to the immune synapse was calculated and the lytic granule distance (LGD) to the immune synapse within each NK cell was calculated using Equation A, which measures the shortest distance between a point and a line:

$$LGD = \frac{|X_m(Y_2 - Y_1) - Y_m(X_2 - X_1) + X_2Y_1 - X_1Y_2|}{\sqrt{(Y_2 - Y_1)^2 + (X_2 - X_1)^2}}$$ Equation A:

Where X_m,Y_m are the coordinates of the individual lytic granule centroid, and X_1, Y_1 and X_2, Y_2 are the coordinates of either end of the immune synapse. For granules outside the synapse length, for which Equation A underestimated the distance to the synapse, distance to the nearest synapse endpoint was calculated using Equation B:

$$LGD = \sqrt{(Y_m - Y_1)^2 + (X_m - X_1)^2}$$ Equation B:

Where X_m,Y_m are the coordinates of the individual lytic granule centroid, and X_1,Y_1 are the coordinates of the nearest synapse endpoint (Supplemental Fig. 1).

Lytic granules clustered closely together could not be adequately resolved into distinct individual granules by ImageJ. Thus, some regions of lytic granules comprised several merged granules with a combined larger area of fluorescent signal. To account for differences in the area of lytic granule regions that could bias the overall calculation of granule distance to the synapse, it was necessary to factor granule area in to this calculation (as in (25)). Each granule distance was weighted by the individual lytic granule area relative to the total granule area within each NK cell using Equation C to calculate the area-weighted mean lytic granule distance (AWMLGD) in μm:

$$AWMLGD = \sum_{i=1}^{n} \frac{LGD_i * A_i}{A_{total}}$$ Equation C:

Where LGD_i is the lytic granule distance of an individual lytic granule calculated using Equation A or B, A_i is the area of the individual lytic granule, and A_{total} is the total area of all lytic granules within an NK cell. The AWMLGD is then the summation of the area-weighted lytic granule distances of n lytic granules within one NK cell (numbered i=1 to i=n). If the AWMLGD to the synapse was < 2 μm, that individual NK cell's lytic granules were considered polarized to the target cell immune synapse. AWMLGD < 2 μm is consistent with a length less than one-third the distance between the target cell immune synapse and the opposite border of the NK cell which has also been used to define human NK cell lytic granule polarization (26).

Cytoskeletal protein array

NK cells were exposed to vehicle, dexamethasone, or LXA_4 for 48 hours as above and cryopreserved. Protein was extracted from thawed NK cells in radioimmunoprecipitation assay (RIPA) buffer (Boston BioProducts) with protease inhibitors (Roche). NK cell lysates were pooled from 9 donors for each condition and an antibody array was used to assess a panel of cytoskeletal proteins (Cytoskeleton Phospho Antibody Array, Full Moon Biosystems) using the manufacturer's recommended protocol. In brief, 50 μg of protein

lysate from each condition was biotinylated and conjugated to a pre-prepared array slide with covalently immobilized antibodies (Cytoskeleton Phospho Antibody Array, Full Moon Biosystems). Slides were incubated with Cy3-streptavidin and imaged on a microarray scanner. Slides comprised 141 site-specific and phospho-specific antibodies with 6 replicates per antibody and positive and negative controls. Mean signal intensity of replicates was calculated for each protein and threshold for detection was defined as twice the background intensity (empty spots). To normalize for small differences in background amongst slides, background intensity was subtracted from mean signal intensity for each protein for each slide. For the 13 proteins above the limits of detection in all conditions, the expression relative to vehicle control was calculated for the LXA_4 and dexamethasone conditions.

Western blotting

NK cell lysates were resolved in denaturing SDS-PAGE conditions by 4–20% Mini-PROTEAN TGX gel (Bio-Rad) and transferred to polyvinylidene difluoride membranes (Bio-Rad). Membranes were blocked with 5% skim milk, incubated with primary antibody at 4°C overnight, followed by secondary antibody (goat anti-rabbit HRP; Cell Signaling Technology) for 1 hour at room temperature. Immunoblots were incubated with SuperSignal West Femto substrate (Thermo Scientific) for 5 minutes and imaged using a Bio-Rad ChemiDoc XRS. Primary antibodies included: from Invitrogen: anti-p-LIMK1 (Thr508); anti-GAPDH; and from Cell Signaling Technology: anti-LIMK1 (3842); anti-LIMK2 (8C11); anti-p-cofilin (Ser3) (77G2); anti-cofilin (D3F9) XP. LIMK1 and LIMK2 antibodies do not cross-react with the other isoform. Densitometry was performed using ImageJ (Fiji; NIH). Protein levels were normalized to GAPDH loading control and fold difference relative to vehicle was calculated for each condition.

LIMK inhibition

In select experiments, NK cells were exposed to the LIMK inhibitor BMS-5 (Enzo Life Sciences) at 1 μM, 5 μM, or 10 μM for 48 hours. Vehicle was 0.02% DMSO. In indicated experiments, NK cells were exposed to BMS-5 10 μM for 15 minutes prior to LXA_4 (100 nM). BMS-5 and LXA_4 were re-dosed at 24 hours.

Confocal microscopy

NK cells were exposed to noted conditions for 48 hours prior to exposure to target K562 cells for 2 hours. Co-cultures were transferred to slides for adhesion, fixation, permeabilization, and blocking as in “Immunofluorescence Microscopy”. Slides were incubated with AlexaFluor 488-human anti-perforin (dG9; BioLegend) and AlexaFluor 647 human anti-α-tubulin (11H10; Cell Signaling Technology) in antibody buffer (PBS with 1% BSA and 0.3% TritonX100) for 45 minutes at 37°C followed by AlexaFluor 555-phalloidin (Cell Signaling Technology) for 15 minutes at room temperature to detect F-actin. Slides were mounted with 0.15mm coverslips using ProLong Gold with DAPI (Invitrogen). Images were acquired in a single z-plane using an Olympus Fluoview FV10i laser scanning confocal microscope with a 60X 1.35 numerical aperture water immersion objective with 6X additional optical zoom. Excitation was with 405, 473, 559, and 635nm ultraviolet/visible light diode lasers and detection was with a variable barrier filter set for optimal wavelengths for fluorophores. ImageJ (Fiji, NIH) was used to quantify F-actin and perforin density at

immune synapse and MTOC to synapse distance (Supplemental Fig. 1F–G). In brief, the immune synapse was identified as the overlap of perimeters of an NK cell and target cell. To measure F-actin accumulation at the immune synapse, phalloidin area (μm^2) and mean fluorescence intensity (MFI) above that of a background threshold was measured within the immune synapse region. F-actin density was defined as the product of the area and MFI of phalloidin signal within the synapse region. The NK cell MTOC was identified as the point of brightest intensity of α-tubulin signal within the NK cell and the centroid coordinates were noted. The distance between the NK cell MTOC and the center of the immune synapse, as defined by the centroid of the phalloidin fluorescence intensity, was measured in each NK:target conjugate (Supplemental Fig. 1F–G). Perforin density at the immune synapse was measured by calculating the product of the MFI and area of perforin signal above background threshold within the defined immune synapse region (Supplemental Fig. 1F–G). Total NK cell perforin density was also calculated in the same manner. Images presented in figures are the raw acquired images and were not enhanced or manipulated after acquisition.

Statistical Analysis

Data are expressed as mean ± SEM with individual data points or as violin plots with frequency distribution, median and quartiles, and individual data points. Normally distributed data were assessed by two-tailed Student's t-test or one-way analysis of variance (ANOVA) with Tukey's or Holm-Sidak multiple comparisons test. Nonparametric data were assessed using Mann Whitney test. Correlations were evaluated by Pearson correlation coefficient (r). log(Dex) and log(LXA_4) concentration response curves were generated and nonlinear regression was performed using least squares regression fitting method to calculate the half maximal inhibitory concentration (IC50) for dexamethasone with R^2 goodness of fit calculated. $p<0.05$ was considered significant. Data was analyzed with Prism 8.0 (GraphPad).

Results

NK cell cytotoxicity and lytic granule polarization is differentially regulated by dexamethasone and LXA_4

Given the frequent clinical use of corticosteroids and their potential adverse effects on NK cells (12, 14, 15), we assessed the impact of the glucocorticoid dexamethasone on NK cell effector function. NK cells were isolated from healthy subjects, exposed to dexamethasone (1 μM), LXA_4 (100 nM), or vehicle control (0.1% ethanol) for 48 hours prior to co-culture with K562 myeloid tumor cells (NK:target cell ratio 5:1) for 4 hours (Fig. 1). The SPM LXA_4 was chosen based on its capacity to enhance NK cell cytotoxicity (9, 12). K562 target cell apoptosis was determined by flow cytometry staining for annexin V and 7-aminoactinomycin D (7-AAD) (Fig. 1A). NK cells increased target cell apoptosis from 18 ± 1% to 52 ± 4% ($p<0.005$) (Fig. 1B). Exposure to dexamethasone significantly decreased NK cell-mediated cytotoxicity (30 ± 3%; $p<0.005$), a 65% inhibition relative to vehicle (Fig. 1B). In sharp contrast, LXA_4 enhanced NK cell cytotoxicity, inducing apoptosis of 62 ± 5% of target cells ($p<0.005$), a 30% increase relative to vehicle (Fig. 1B). Dexamethasone effectively suppressed NK cell cytotoxicity at even lower concentrations than 1 μM with a calculated half maximal inhibitory concentration (IC50) of 1.7 nM (Supplemental Fig. 2A).

LXA_4 had a similar effect on NK cell cytotoxicity at concentrations between 100pM to 100nM (Supplemental Fig. 2B). Expression of NK cell activating receptors was altered from baseline after 48 hours of *in vitro* culture. Surface expression of NKp46 (Supplemental Fig. 2C) and NKG2D (Supplemental Fig. 2D) proteins were both lower in dexamethasone-exposed NK cells relative to vehicle control, consistent with prior reports for both human and murine NK cells exposed to corticosteroids *in vitro* (18, 19, 27). In contrast, NKp46 and NKG2D expression was preserved in LXA_4-exposed NK cells with surface levels equivalent to vehicle-exposed NK cells (Supplemental Fig. 2C–D).

To determine whether NK cell lytic granule trafficking was impacted by dexamethasone or LXA_4, NK cells were exposed to target cells for 2 hours and intracellular perforin was visualized by immunofluorescence microscopy (Fig. 1C, perforin (green)). ~60% of NK cells formed an immune synapse with a target cell and the frequency of NK:target cell conjugate formation was not significantly changed by exposure to dexamethasone or LXA_4. NK:target cell conjugates had variation in perforin proximity to the synapse (Fig. 1C–E). Individual perforin$^+$ lytic granules were identified within each NK cell and the distance of each lytic granule to the immune synapse was measured. The mean area-weighted lytic granule distance to the immune synapse was calculated for ≥ 45 NK:target interactions in each treatment condition (Fig. 1D; Supplemental Fig. 1). With vehicle control, the median value for the calculated mean lytic granule distance to the immune synapse was 2 μm (Fig. 1D). Lytic granules in dexamethasone-exposed NK cells were farther from the synapse than control (median 2.7 μm; Fig. 1D). In contrast, LXA_4-exposed NK cell lytic granules were closer to the synapse than vehicle (median 1.4 μm, Fig. 1D). Frequency distribution analysis revealed that the largest number of LXA_4-exposed NK cells had lytic granules less than 1 μm from the synapse (Fig. 1E). The distribution of vehicle- and dexamethasone-treated NK cells was broader than LXA_4 with the peak lytic granule distance with dexamethasone shifted further away from the synapse (Fig. 1E, peak bin 2–3 μm). NK cells were defined as having lytic granules polarized to the target cell immune synapse if the area-weighted mean lytic granule distance was <2 μm from the immune synapse (Supplemental Fig. 1). With vehicle, 48 ± 5% of NK cells were polarized (Fig. 1F; n=3). In contrast, dexamethasone impaired NK cell polarization (32 ± 8% polarized) and LXA_4 enhanced polarization (61 ± 9% polarized) (Fig. 1F).

Dexamethasone and LXA_4 regulate NK cell cytoskeletal proteins

Because dexamethasone and LXA_4 had contrasting actions on the NK cell lytic granule distance from the immune synapse, we next screened NK cell cytoskeletal proteins for differential regulation by these stimuli. Of the 141 site-specific and phosphorylation-specific cytoskeleton-targeted proteins screened, 15 were detectable in vehicle-exposed NK cells, 35 in dexamethasone-exposed NK cells, and 97 in LXA_4-exposed NK cells (Supplemental Table 1; Fig. 2A). 13 cytoskeleton proteins were above the limits of detection in NK cells exposed to vehicle, dexamethasone, or LXA_4 (Fig. 2A–B). In addition, p-LIMK1 (Thr508) was detected in vehicle and LXA_4 conditions but was undetectable in dexamethasone-exposed NK cells (Fig. 2A). Several proteins were upregulated at least 2-fold by LXA_4 including FAK, VASP, Src and LIMK 1/2 (Fig. 2B). In contrast, several proteins were downregulated by dexamethasone, including LIMK 1/2 that was suppressed 50% relative to

vehicle (Fig. 2A). Given that dexamethasone and LXA_4 had differential effects on LIMK 1/2 and p-LIMK1 in this screening assay, we chose to focus on the LIMK pathway. LIMK1 and LIMK2 are distinct proteins in the LIM kinase family (28), which were not independently assessed in the screening array, so we next determined the effects of dexamethasone and LXA_4 on each LIMK protein. Consistent with the screening array, LIMK1 expression was inhibited by dexamethasone and increased by LXA_4 in NK cells (Fig. 2C). Distinct from the screening array, p-LIMK1 was detectable in all three conditions by Western blot with a trend for downregulation by dexamethasone and upregulation by LXA_4 (Fig. 2D). LIMK2 expression was suppressed by dexamethasone by 50% (Fig. 2E). In contrast, LIMK2 expression was significantly upregulated by LXA_4 with a mean 4-fold increase relative to vehicle (Fig. 2E). Activated LIMK proteins inhibit the actin depolymerization activity of cofilin by phosphorylation at the amino-terminal Ser3 residue of cofilin (29, 30), so we next assessed whether dexamethasone or LXA_4 exposure changed cofilin expression. There was a strong trend for inhibition of p-cofilin by dexamethasone and for increased total cofilin (Fig. 2F) and p-cofilin (Fig. 2G) by LXA_4.

LIMK inhibition impairs NK cell cytotoxicity

Because dexamethasone and LXA_4 differentially regulated the LIMK proteins in NK cells, we next evaluated whether LIMK activity was necessary for NK cell cytotoxicity. Primary human NK cells were exposed to BMS-5, a specific small molecule inhibitor of LIMK1 and LIMK2, at 1 to 10 μM for 48 hours. Exposure to BMS-5 did not impair NK cell viability over 48 hours (Supplemental Fig. 3A–B). NK cell exposure to BMS-5 reduced LIMK1 (Fig. 3A) and LIMK2 (Fig. 3B) protein levels at all concentrations tested. With 10 μM BMS-5 exposure, NK cell LIMK1 expression was reduced by 45 ± 3% (Fig. 3A; $p<0.005$) and LIMK 2 expression was reduced by 61 ± 2% (Fig. 3B; $p<0.005$). BMS-5 also inhibited p-cofilin expression by 30 ± 9% (Fig. 3C; $p<0.05$) with a trend to decreased expression of total cofilin (Fig. 3D; $p=0.06$). To assess whether inhibiting LIMK impacted NK cell cytotoxicity, BMS-5-exposed NK cells were co-cultured with K562 target cells and target cell apoptosis was determined by flow cytometry staining for annexin V and 7-AAD (Fig. 3E). LIMK inhibition reduced NK cell-mediated target cell apoptosis from 48 ± 3% in vehicle to 33 ± 2% in NK cells exposed to 10 μM BMS-5, a ~30% inhibition of target cell killing (Fig. 3F; $p<0.05$).

LIMK inhibition disrupts synaptic F-actin accumulation and MTOC polarization

Because the LIMK proteins regulate actin polymerization and microtubule dynamics (29–31), we hypothesized that inhibiting LIMK would disrupt assembly of the NK:target immune synapse and NK cell MTOC polarization. We utilized confocal microscopy to study intracellular cytoskeletal rearrangement and lytic granule localization in NK cells engaged with K562 target cells (Fig. 4, Supplemental Fig. 1, Supplemental Fig. 4). NK cells were exposed to the LIMK inhibitor BMS-5 or DMSO control for 48 hours followed by co-culture with K562 target cells for 2 hours. Intracellular F-actin, α-tubulin, and perforin were evaluated in NK:target interactions (Fig. 4A, Supplemental Fig. 4). Exposure to BMS-5 did not impair NK cell conjugate formation with target cells (Supplemental Fig. 3C). Of note, there was less F-actin accumulation at the immune synapse in BMS-5-exposed NK cells (Fig. 4A, Supplemental Fig. 4; phalloidin (red)). F-actin accumulation at the immune

synapse was quantified by measuring the area (Fig. 4B) and mean fluorescence intensity (MFI; Fig. 4C) of F-actin within the immune synapse (see Methods in Supplemental Fig. 1F–G). F-actin area, MFI, and integrated density (product of area and MFI) within the NK:target immune synapse were all significantly reduced in a dose-dependent fashion by BMS-5 (Fig. 4A–D). BMS-5 exposure reduced the accumulation of F-actin at the NK cell immune synapse by 7-fold (median F-actin integrated density 230 au for DMSO relative to 31 au for 10 μM BMS-5; $p<0.0001$; Fig. 4D).

We next identified the NK cell MTOC as a discrete α-tubulin signal and measured the distance from the MTOC to the immune synapse using confocal microscopy (see Methods in Supplemental Fig. 1F–G). MTOC polarization to the synapse was inhibited in a dose-dependent fashion by BMS-5 (Fig. 4A, 4E). The MTOC to synapse distance was much farther in BMS-5 exposed NK cells, 2.8 μm and 3.2 μm (in 5 μM and 10 μM BMS-5 conditions respectively), compared to 1.5 μm for vehicle control (Fig. 4E, $p<0.005$). There was an inverse correlation between synaptic F-actin density and MTOC to synapse distance (Fig. 4F; Pearson $r = -0.33$, $p=0.0002$), indicative of an association between reduced F-actin accumulation at the immune synapse and impaired MTOC polarization. NK cell lytic granules were identified by perforin fluorescence (Fig. 4A; green). BMS-5 exposure did not reduce the total perforin content of NK cells (Supplemental Fig. 3D). BMS-5 altered NK cell lytic granule distribution resulting in a dispersed granule pattern that was farther from the target cell interface (Fig. 4A). The density of perforin$^+$ lytic granules within the target cell immune synapse was significantly reduced in BMS-5-exposed NK cells (Fig. 4G; median 37 au (DMSO), 10 au (BMS-5 5 μM) and 0 (BMS-5 10 μM); $p<0.0005$).

Dexamethasone and LXA_4 differentially regulate NK cell cytoskeletal rearrangement

Because dexamethasone suppressed and LXA_4 increased LIMK expression in NK cells (Fig. 2) and LIMK inhibition disrupted F-actin accumulation and MTOC polarization to the immune synapse and NK cell cytotoxicity (Fig. 3 and Fig. 4), we next investigated the effects of dexamethasone and LXA_4 on NK cell cytoskeletal rearrangement. NK cells were exposed to dexamethasone (1 μM), LXA_4 (100 nM), or vehicle (0.1% EtOH) for 48 hours prior to co-culture with K562 target cells for 2 hours and intracellular F-actin, perforin, and α-tubulin were evaluated with confocal microscopy (Fig. 5A). F-actin density at the NK:target immune synapse in dexamethasone-exposed NK cells was < 50% that of vehicle (median F-actin density 157 au (Dex) versus 383 au (Veh); Fig. 5B; $p<0.0001$). In contrast, accumulation of F-actin at the NK:target immune synapse was preserved in LXA_4-exposed NK cells (Fig. 5B; median F-actin density 389 au). Perforin$^+$ lytic granules converged at the MTOC in dexamethasone-exposed NK cells; however, the MTOC/lytic granule complex remained remote from the synapse in many cells (Fig 5A). The MTOC to synapse distance was significantly farther in dexamethasone-exposed NK cells (median 3.6 μm) than vehicle-exposed cells (median 1.9 μm) (Fig. 5C; $p<0.0001$). The median MTOC to synapse distance in LXA_4-exposed NK cells was 1.4 μm, significantly shorter than in dexamethasone-exposed cells (Fig. 5C; $p<0.0001$) with a trend to shorter than vehicle control. The MTOC to synapse distance was inversely correlated with F-actin density at the immune synapse when NK cells from all treatment conditions were compiled (Fig. 5D; Pearson $r = -0.22$, $p=0.0088$). Notably, the proportion of NK cells with the MTOC polarized to the synapse (defined as

MTOC to synapse distance <2 μm) differed amongst conditions. Only 18% of dexamethasone-exposed NK cells had the MTOC polarized compared to 57% in vehicle control (Fig. 5E). Enhanced MTOC polarization was noted in LXA_4-exposed NK cells where 65% were polarized (Fig. 5E). The density of perforin$^+$ lytic granules within the NK:target cell immune synapse (Fig. 5F) and in the entire NK cell (Fig. 5G) was significantly reduced in dexamethasone-exposed NK cells relative to vehicle- or LXA_4-exposed NK cells.

LXA_4 effect on NK cells is abrogated by LIMK inhibition

Given our findings that LIMK is necessary for NK cell cytoskeletal rearrangement (Fig. 4) and because LXA_4 increased the expression of LIMK in NK cells (Fig. 2) and augmented NK cell cytotoxicity (Fig. 1), we next assessed whether LIMK inhibition impacted LXA_4's actions on NK cells. NK cells pre-treated with the LIMK inhibitor BMS-5 prior to LXA_4 exposure had altered cytoskeletal rearrangement (Fig. 5A). LIMK inhibition, even in the presence of LXA_4, reduced the synaptic accumulation of F-actin (Fig. 5H), impaired MTOC polarization to the target cell synapse (Fig. 5I), and prevented perforin$^+$ lytic granule delivery to the synapse (Fig. 5J). Furthermore, BMS-5 reduced the cytotoxicity of LXA_4-exposed NK cells by ~30% from 74 ±1% target cell apoptosis to 52 ± 3% (Fig. 5K; $p<0.005$). NK cells exposed to LXA_4 in the presence of BMS-5 had reduced expression of LIMK1, LIMK2, p-cofilin, and total cofilin by Western immunoblotting (Fig. 5L).

Discussion

NK cells are sentinel cytotoxic innate lymphocytes that rapidly recognize and kill abnormal or infected cells to protect the host against viruses and malignancy (1, 2). NK cells are equipped with pre-formed lytic granules containing perforin and granzymes that activate target cell apoptosis. Cytoskeletal rearrangements must be orchestrated for NK cell recognition, engagement, and killing of target cells through directed exocytosis of lytic granules (3, 4). Here, we have identified the family of LIM kinases as central regulators of the cytoskeletal changes needed for NK cell immune synapse formation, lytic granule trafficking, and cytotoxicity. Of clinical relevance, the glucocorticoid dexamethasone decreased LIMK expression in NK cells and inhibited NK cell cytotoxicity. In contrast, the SPM LXA_4 increased NK cell LIMK expression to facilitate F-actin anchoring for maturation of the immune synapse, lytic granule trafficking, and efficient cytotoxicity.

Dexamethasone had a marked effect on NK cell lytic granule trafficking to the interface with target cells, decreased accumulation of F-actin at the immune synapse, and compromised cytotoxicity. NK cells formation of conjugates with target cells was not adversely impacted by dexamethasone, so its suppression of NK cell killing was downstream of target recognition. In contrast to corticosteroids, SPMs increase NK cell cytotoxicity (8, 9, 12). LXA_4 is the lead SPM and its actions promote resolution of inflammation to restore inflamed tissues to homeostasis (10, 11). The LXA_4 cognate receptor ALX/FPR2 is expressed on NK cells (9, 12). LXA_4 can increase NK cell-directed apoptosis of activated granulocytes and lymphocytes to promote lung inflammation resolution (8, 9). Here, in contrast to dexamethasone, LXA_4 enhanced NK cell cytotoxicity by promoting intracellular

lytic granule trafficking to the target cell immune synapse and synaptic accumulation of F-actin to promote a mature lytic synapse. These results emphasize the distinction between anti-inflammation and pro-resolution and indicate that glucocorticoids disrupt NK cell cytotoxicity.

NK cell-directed apoptosis is a multi-stage process. Intracellular lytic granules are delivered to the NK:target immune synapse where perforin forms pores in the target cell membrane and granzymes are exocytosed to trigger apoptosis (32). The intracellular movement of NK cell lytic granules requires coordinated rearrangement of the cytoskeleton (3, 4). Dexamethasone and LXA_4 had opposing actions on NK cell cytotoxicity and differentially regulated cytoskeletal protein expression. The induction of LIMK by LXA_4 and their suppression by dexamethasone suggested a pivotal role for these proteins. LIMK are serine/threonine kinases that operate downstream of RhoA-family GTPases that phosphorylate and activate LIMK (33, 34). LXA_4 induced p-LIMK1, which phosphorylates cofilin to stop cofilin-induced actin depolymerization. Cofilin regulation is essential in facilitating the dynamic filamentous actin reorganization necessary for basic cellular functions, such as motility and division (29, 30). LIMK1 knockout mice display neurologic and developmental abnormalities related to aberrant cytoskeletal dynamics (35). To date, there are no reports of NK cell or immune system alterations in LIMK-deficient animals. Here, LIMK activity was necessary for human NK cell cytotoxicity, as inhibition of LIMK1 and LIMK2 with BMS-5 prevented accumulation of F-actin at the NK:target immune synapse, inhibited polarization of lytic granules and MTOC to the synapse, and impeded target cell killing. These findings support the importance of the RhoA/ROCK/LIMK pathway in cytotoxic lymphocyte polarization and killing (36). BMS-5 suppressed NK cell p-cofilin as anticipated, but also reduced LIMK1 and LIMK2. These data suggest that pharmacologic inhibition of LIMK may also regulate expression of the parent protein and downstream signaling pathway proteins to disable NK cell cytotoxicity.

LIMK activity was necessary for LXA_4's actions on NK cell function, as LIMK inhibition with BMS-5 impaired LXA_4 induction of NK cell synaptic accumulation of F-actin, polarization of the MTOC, trafficking of perforin$^+$ lytic granules to the synapse, and cytotoxicity. LXA_4 and LXA_4 stable analogues may share signal transduction pathways for cytoskeletal rearrangement in other cell types. For example, LXA_4 induces actin reorganization in macrophages, at least in part through upregulation of RhoA activity, which enhances macrophage filopodia and lamellipodia formation and promotes phagocytosis (37). These mechanisms appear to be active in SPM-driven resolution of tumor debris and associated inflammation (38, 39). Of note, RhoA is upstream of LIMK activation (33, 34), suggesting that LXA_4 regulation of the NK cell RhoA/LIMK pathway is a more generalizable mechanism of action for signal transduction and cytoskeletal rearrangement in diverse cell types.

There are some limitations to our study. It is likely that glucocorticoids also suppress other signaling pathways aside from LIMK that are critical for effective NK cell cytotoxicity. Steroid-induced down-regulation of natural cytotoxicity receptors (*e.g.* NKp46) and activating receptors, such as NKG2D, would also hinder the appropriate signaling cascades needed to trigger NK cell activation and target cell killing. Future studies are warranted to

evaluate whether mediators such as LXA_4 could blunt glucocorticoid-mediated down-regulation of pivotal NK cell activating proteins and signaling pathways. Emerging evidence suggests that *in vitro* cytokine activation of human NK cells with IL-12, IL-15, and IL-18 generates a memory-like NK cell phenotype with enhanced cytotoxicity and IFN-γ production (40, 41). Of interest, the immunosuppressive effects of dexamethasone on NK cells have recently been described to be regulated by concomitant exposure to specific cytokine combinations (*i.e.* IL-2 and IL-12) (18). Further study is needed to examine whether *in vitro* exposure to select cytokines influences LXA_4 or dexamethasone effects on NK cell LIMK expression, cytoskeletal dynamics, and cytotoxicity.

In summary, we have identified the activation of LIMK as an important regulator of cytoskeletal rearrangement in NK cells for cytotoxicity of target cells. The glucocorticoid dexamethasone inhibited LIMK and, similar to the LIMK inhibitor BMS-5, impaired cytotoxicity of NK cells. Increased LIMK activity induced by the SPM LXA_4 enhanced NK cell cytoskeletal rearrangement to polarize the MTOC and lytic granules closer to the immune synapse for more effective cytotoxicity. The immunosuppressive effects of corticosteroids on NK cells may not have been fully appreciated and the results presented here suggest that their use be scrutinized in conditions where NK cells serve as vital cellular effectors for the resolution of inflammation, including host responses to severe viral infections and cancer.

Supplementary Material

Refer to Web version on PubMed Central for supplementary material.

Acknowledgements

We thank the members of the Levy laboratory for constructive discussions and critical review of the manuscript.

Funding: This study was conducted with the support of grants awarded by the National Institutes of Health including R01-HL122531 (BDL), P01-GM095467 (Project 2; BDL), K12-HD047349 (MGD), and K08-HL145098 (MGD).

References

1. Vivier E, Raulet DH, Moretta A, Caligiuri MA, Zitvogel L, Lanier LL, Yokoyama WM, and Ugolini S. 2011 Innate or adaptive immunity? The example of natural killer cells. Science 331: 44–49. [PubMed: 21212348]
2. Caligiuri MA 2008 Human natural killer cells. Blood 112: 461–469. [PubMed: 18650461]
3. Mace EM, Dongre P, Hsu HT, Sinha P, James AM, Mann SS, Forbes LR, Watkin LB, and Orange JS. 2014 Cell biological steps and checkpoints in accessing NK cell cytotoxicity. Immunol Cell Biol 92: 245–255. [PubMed: 24445602]
4. Orange JS 2008 Formation and function of the lytic NK-cell immunological synapse. Nat Rev Immunol 8: 713–725. [PubMed: 19172692]
5. Mace EM, and Orange JS. 2014 Lytic immune synapse function requires filamentous actin deconstruction by Coronin 1A. Proc Natl Acad Sci U S A 111: 6708–6713. [PubMed: 24760828]
6. Orange JS, Ramesh N, Remold-O'Donnell E, Sasahara Y, Koopman L, Byrne M, Bonilla FA, Rosen FS, Geha RS, and Strominger JL. 2002 Wiskott-Aldrich syndrome protein is required for NK cell cytotoxicity and colocalizes with actin to NK cell-activating immunologic synapses. Proc Natl Acad Sci U S A 99: 11351–11356. [PubMed: 12177428]

7. Zhang Q, Davis JC, Lamborn IT, Freeman AF, Jing H, Favreau AJ, Matthews HF, Davis J, Turner ML, Uzel G, Holland SM, and Su HC. 2009 Combined immunodeficiency associated with DOCK8 mutations. N Engl J Med 361: 2046–2055. [PubMed: 19776401]
8. Haworth O, Cernadas M, and Levy BD. 2011 NK cells are effectors for resolvin E1 in the timely resolution of allergic airway inflammation. J Immunol 186: 6129–6135. [PubMed: 21515793]
9. Barnig C, Cernadas M, Dutile S, Liu X, Perrella MA, Kazani S, Wechsler ME, Israel E, and Levy BD. 2013 Lipoxin A4 regulates natural killer cell and type 2 innate lymphoid cell activation in asthma. Sci Transl Med 5: 174ra126.
10. Serhan CN 2014 Pro-resolving lipid mediators are leads for resolution physiology. Nature 510: 92–101. [PubMed: 24899309]
11. Serhan CN, and Levy BD. 2018 Resolvins in inflammation: emergence of the pro-resolving superfamily of mediators. J Clin Invest 128: 2657–2669. [PubMed: 29757195]
12. Duvall MG, Barnig C, Cernadas M, Ricklefs I, Krishnamoorthy N, Grossman NL, Bhakta NR, Fahy JV, Bleecker ER, Castro M, Erzurum SC, Gaston BM, Jarjour NN, Mauger DT, Wenzel SE, Comhair SA, Coverstone AM, Fajt ML, Hastie AT, Johansson MW, Peters MC, Phillips BR, Israel E, Levy BD, and the National Heart, Lung, and Blood Institute's Severe Asthma Research Program-3 Investigators. 2017 Natural killer cell-mediated inflammation resolution is disabled in severe asthma. Sci Immunol 2: eaam5446. [PubMed: 28783702]
13. Levy BD, Bonnans C, Silverman ES, Palmer LJ, Marigowda G, Israel E, Severe NHL Asthma Research Program, and I. Blood. 2005 Diminished lipoxin biosynthesis in severe asthma. Am J Respir Crit Care Med 172: 824–830. [PubMed: 15961693]
14. Pedersen BK, and Beyer JM. 1986 Characterization of the in vitro effects of glucocorticosteroids on NK cell activity. Allergy 41: 220–224. [PubMed: 2424334]
15. Di Lorenzo G, Esposito Pellitteri M, Drago A, Di Blasi P, Candore G, Balistreri C, Listi F, and Caruso C. 2001 Effects of in vitro treatment with fluticasone propionate on natural killer and lymphokine-induced killer activity in asthmatic and healthy individuals. Allergy 56: 323–327. [PubMed: 11284800]
16. Holbrook NJ, Cox WI, and Horner HC. 1983 Direct suppression of natural killer activity in human peripheral blood leukocyte cultures by glucocorticoids and its modulation by interferon. Cancer Res 43: 4019–4025. [PubMed: 6871844]
17. Hsu AK, Quach H, Tai T, Prince HM, Harrison SJ, Trapani JA, Smyth MJ, Neeson P, and Ritchie DS. 2011 The immunostimulatory effect of lenalidomide on NK-cell function is profoundly inhibited by concurrent dexamethasone therapy. Blood 117: 1605–1613. [PubMed: 20978269]
18. Morgan DJ, and Davis DM. 2017 Distinct Effects of Dexamethasone on Human Natural Killer Cell Responses Dependent on Cytokines. Front Immunol 8: 432. [PubMed: 28450865]
19. Vitale C, Chiossone L, Cantoni C, Morreale G, Cottalasso F, Moretti S, Pistorio A, Haupt R, Lanino E, Dini G, Moretta L, and Mingari MC. 2004 The corticosteroid-induced inhibitory effect on NK cell function reflects down-regulation and/or dysfunction of triggering receptors involved in natural cytotoxicity. Eur J Immunol 34: 3028–3038. [PubMed: 15368269]
20. Chiurchiu V, Leuti A, Dalli J, Jacobsson A, Battistini L, Maccarrone M, and Serhan CN. 2016 Proresolving lipid mediators resolvin D1, resolvin D2, and maresin 1 are critical in modulating T cell responses. Sci Transl Med 8: 353ra111.
21. Maddox JF, Hachicha M, Takano T, Petasis NA, Fokin VV, and Serhan CN. 1997 Lipoxin A4 stable analogs are potent mimetics that stimulate human monocytes and THP-1 cells via a G-protein-linked lipoxin A4 receptor. J Biol Chem 272: 6972–6978. [PubMed: 9054386]
22. Maddox JF, and Serhan CN. 1996 Lipoxin A4 and B4 are potent stimuli for human monocyte migration and adhesion: selective inactivation by dehydrogenation and reduction. J Exp Med 183: 137–146. [PubMed: 8551217]
23. Ramstedt U, Ng J, Wigzell H, Serhan CN, and Samuelsson B. 1985 Action of novel eicosanoids lipoxin A and B on human natural killer cell cytotoxicity: effects on intracellular cAMP and target cell binding. J Immunol 135: 3434–3438. [PubMed: 2995494]
24. Ramstedt U, Serhan CN, Nicolaou KC, Webber SE, Wigzell H, and Samuelsson B. 1987 Lipoxin A-induced inhibition of human natural killer cell cytotoxicity: studies on stereospecificity of inhibition and mode of action. J Imunol 138: 266–270.

25. Mentlik AN, Sanborn KB, Holzbaur EL, and Orange JS. 2010 Rapid lytic granule convergence to the MTOC in natural killer cells is dependent on dynein but not cytolytic commitment. Mol Biol Cell 21: 2241–2256. [PubMed: 20444980]
26. Hsu HT, Mace EM, Carisey AF, Viswanath DI, Christakou AE, Wiklund M, Onfelt B, and Orange JS. 2016 NK cells converge lytic granules to promote cytotoxicity and prevent bystander killing. J Cell Biol 215: 875–889. [PubMed: 27903610]
27. Chen L, Jondal M, and Yakimchuk K. 2018 Regulatory effects of dexamethasone on NK and T cell immunity. Inflammopharmacology 26: 1331–1338. [PubMed: 29159714]
28. Okano I, Hiraoka J, Otera H, Nunoue K, Ohashi K, Iwashita S, Hirai M, and Mizuno K. 1995 Identification and characterization of a novel family of serine/threonine kinases containing two N-terminal LIM motifs. J Biol Chem 270: 31321–31330. [PubMed: 8537403]
29. Yang N, Higuchi O, Ohashi K, Nagata K, Wada A, Kangawa K, Nishida E, and Mizuno K. 1998 Cofilin phosphorylation by LIM-kinase 1 and its role in Rac-mediated actin reorganization. Nature 393: 809–812. [PubMed: 9655398]
30. Arber S, Barbayannis FA, Hanser H, Schneider C, Stanyon CA, Bernard O, and Caroni P. 1998 Regulation of actin dynamics through phosphorylation of cofilin by LIM-kinase. Nature 393: 805–809. [PubMed: 9655397]
31. Prunier C, Prudent R, Kapur R, Sadoul K, and Lafanechere L. 2017 LIM kinases: cofilin and beyond. Oncotarget 8: 41749–41763. [PubMed: 28445157]
32. Thiery J, Keefe D, Boulant S, Boucrot E, Walch M, Martinvalet D, Goping IS, Bleackley RC, Kirchhausen T, and Lieberman J. 2011 Perforin pores in the endosomal membrane trigger the release of endocytosed granzyme B into the cytosol of target cells. Nat Immunol 12: 770–777. [PubMed: 21685908]
33. Edwards DC, Sanders LC, Bokoch GM, and Gill GN. 1999 Activation of LIM-kinase by Pak1 couples Rac/Cdc42 GTPase signalling to actin cytoskeletal dynamics. Nat Cell Biol 1: 253–259. [PubMed: 10559936]
34. Maekawa M, Ishizaki T, Boku S, Watanabe N, Fujita A, Iwamatsu A, Obinata T, Ohashi K, Mizuno K, and Narumiya S. 1999 Signaling from Rho to the actin cytoskeleton through protein kinases ROCK and LIM-kinase. Science 285: 895–898. [PubMed: 10436159]
35. Meng Y, Zhang Y, Tregoubov V, Janus C, Cruz L, Jackson M, Lu WY, MacDonald JF, Wang JY, Falls DL, and Jia Z. 2002 Abnormal spine morphology and enhanced LTP in LIMK-1 knockout mice. Neuron 35: 121–133. [PubMed: 12123613]
36. Lou Z, Billadeau DD, Savoy DN, Schoon RA, and Leibson PJ. 2001 A role for a RhoA/ROCK/LIM-kinase pathway in the regulation of cytotoxic lymphocytes. J Immunol 167: 5749–5757. [PubMed: 11698448]
37. Maderna P, Cottell DC, Berlasconi G, Petasis NA, Brady HR, and Godson C. 2002 Lipoxins induce actin reorganization in monocytes and macrophages but not in neutrophils: differential involvement of rho GTPases. Am J Pathol 160: 2275–2283. [PubMed: 12057930]
38. Sulciner ML, Serhan CN, Gilligan MM, Mudge DK, Chang J, Gartung A, Lehner KA, Bielenberg DR, Schmidt B, Dalli J, Greene ER, Gus-Brautbar Y, Piwowarski J, Mammoto T, Zurakowski D, Perretti M, Sukhatme VP, Kaipainen A, Kieran MW, Huang S, and Panigrahy D. 2018 Resolvins suppress tumor growth and enhance cancer therapy. J Exp Med 215: 115–140. [PubMed: 29191914]
39. Gilligan MM, Gartung A, Sulciner ML, Norris PC, Sukhatme VP, Bielenberg DR, Huang S, Kieran MW, Serhan CN, and Panigrahy D. 2019 Aspirin-triggered proresolving mediators stimulate resolution in cancer. Proc Natl Acad Sci U S A 116: 6292–6297. [PubMed: 30862734]
40. Romee R, Rosario M, Berrien-Elliott MM, Wagner JA, Jewell BA, Schappe T, Leong JW, Abdel-Latif S, Schneider SE, Willey S, Neal CC, Yu L, Oh ST, Lee YS, Mulder A, Claas F, Cooper MA, and Fehniger TA. 2016 Cytokine-induced memory-like natural killer cells exhibit enhanced responses against myeloid leukemia. Sci Transl Med 8: 357ra123.
41. Cooper MA, Elliott JM, Keyel PA, Yang L, Carrero JA, and Yokoyama WM. 2009 Cytokine-induced memory-like natural killer cells. Proc Natl Acad Sci U S A 106: 1915–1919. [PubMed: 19181844]

Key Points

- Dexamethasone impairs NK cell cytotoxicity by suppressing LIMK F-actin regulation
- Lipoxin A_4 induces LIMK to promote lytic granule trafficking and NK cell killing

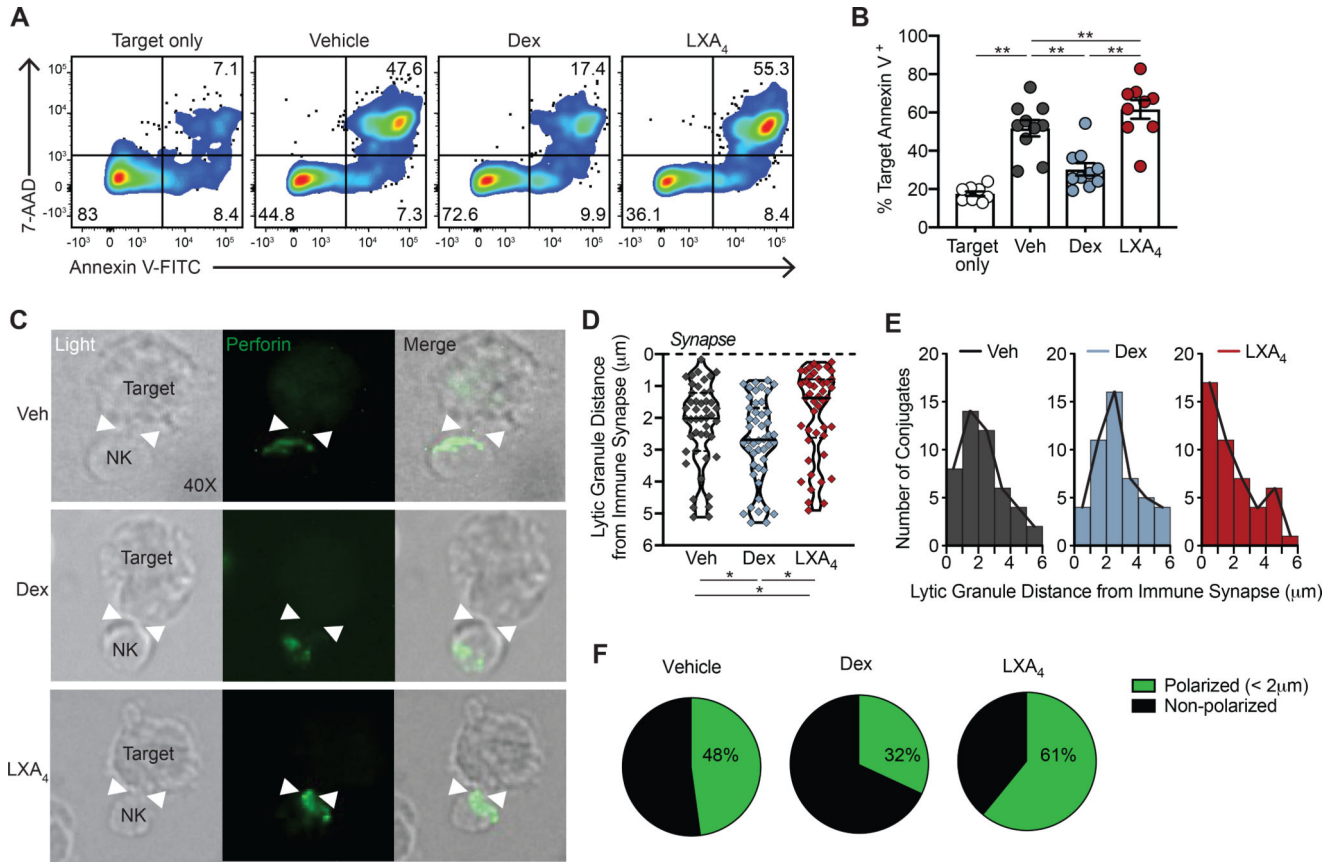

Figure 1. NK cell cytotoxicity and lytic granule polarization is differentially regulated by dexamethasone and LXA_4.

NK cells isolated from healthy donors were exposed to vehicle control (Veh, grey), 1 μM dexamethasone (Dex, blue), or 100 nM lipoxin A_4 (LXA_4, red) for 48 hours. **(A-B)** Treated NK cells were co-incubated with K562 target cells at 5:1 effector:target ratio for 4 hours. **(A)** Target cell apoptosis was assessed by flow cytometry staining for annexin-V and 7-AAD. Quadrant numbers indicate % of target cells. **(B)** Target cell apoptosis (% annexin V^+) was assessed in target cells alone and targets co-incubated with Veh- (grey), Dex- (blue), or LXA_4- (red) exposed NK cells. n=10 experiments. Bars show mean ± SEM with individual data points. **p<0.005 by repeated measures one-way ANOVA with Tukey's multiple comparisons test. **(C-F)** Immunofluorescence microscopy of treated NK cells exposed to K562 target cells for 2 hours. **(C)** NK:target conjugates were identified by light (40X) and the immune synapse with target cells was identified (white arrowheads). Intracellular perforin (AF488, green) identifies NK cell lytic granules. **(D)** The area-weighted mean lytic granule distance from the target cell immune synapse was calculated for an average 4 granules per NK cell. The immune synapse is depicted with a dashed line. Violin plots depict the density distribution of lytic granule distance from the immune synapse (in μm) with median and interquartile ranges for the per-cell calculated means that are shown as individual data points (diamonds). *p<0.05 by Mann-Whitney U test. **(E)** Histograms show the frequency distribution of NK cell area-weighted mean lytic granule distance from immune synapse in each condition. **(F)** Percentage of NK cells with lytic granules polarized

toward the immune synapse (< 2 μm) is compared in each condition. n=3 experiments. ≥ 45 NK:target conjugate images were analyzed per condition.

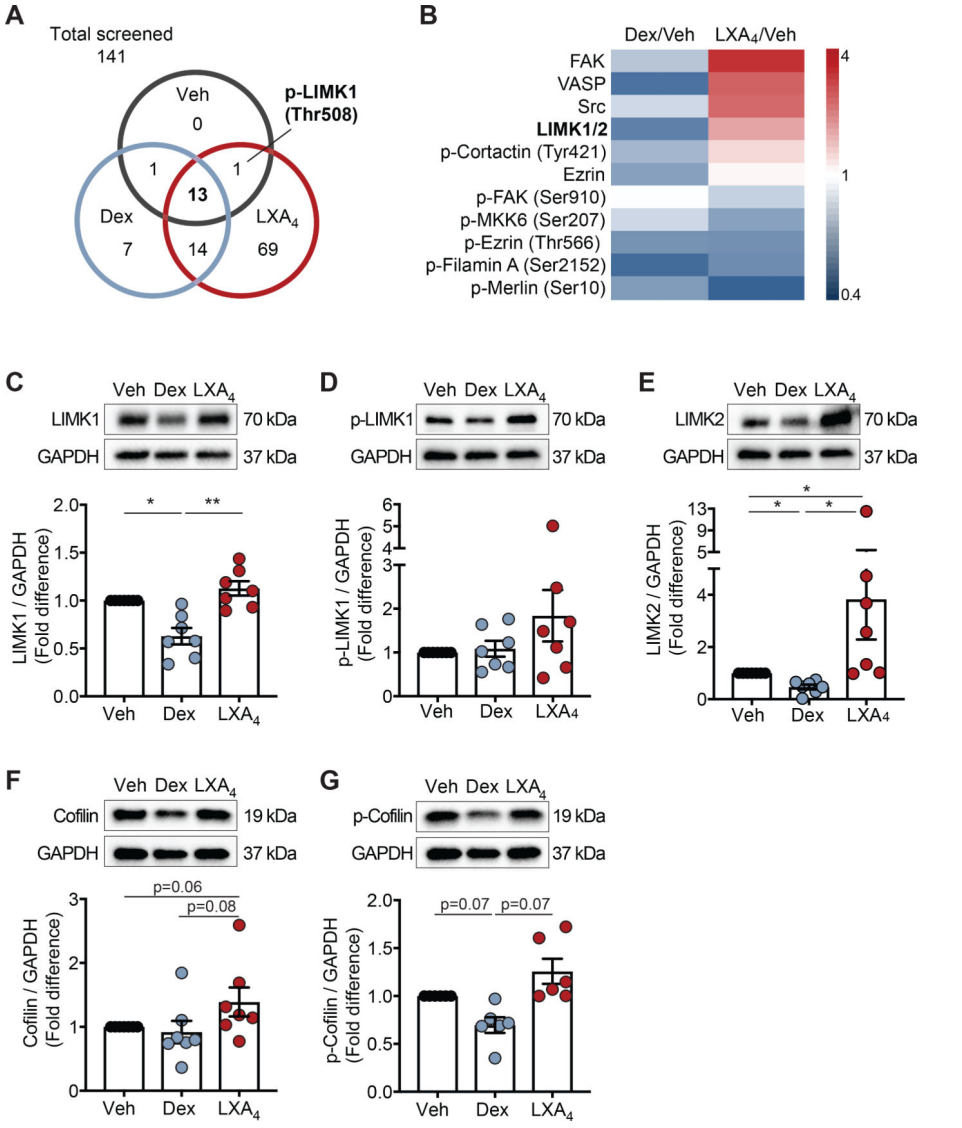

Figure 2. Dexamethasone and LXA_4 regulate NK cell cytoskeletal proteins.

Circulating NK cells from healthy donors were exposed to Veh, Dex, or LXA_4 for 48 hours and protein was extracted. **(A)** Venn diagram depicts the number of cytoskeletal proteins detected in each condition for the 141 site-specific proteins assessed in a screening array. **(B)** For proteins that were detectable in all conditions, the fold-change relative to vehicle was compared for Dex- and LXA_4- exposed NK cells. Heat map displays increased expression (red) and decreased expression (blue) relative to vehicle control. **(C-G)** Protein expression was analyzed by Western immunoblotting of NK cell protein lysates and normalized to GAPDH loading control. Relative expression of **(C)** LIMK1, **(D)** p-LIMK1, **(E)** LIMK2, **(F)** cofilin, and **(G)** p-cofilin was compared for Dex and LXA_4 normalized to vehicle control (n ≥ 6 experiments). 2–5 μg protein extract was loaded per lane; consistent amounts of protein were used within each individual experiment. Bars depict mean ± SEM with individual data points. *p<0.05, **p<0.005 by repeated measures one-way ANOVA with Holm-Sidak multiple comparisons test performed on unscaled data.

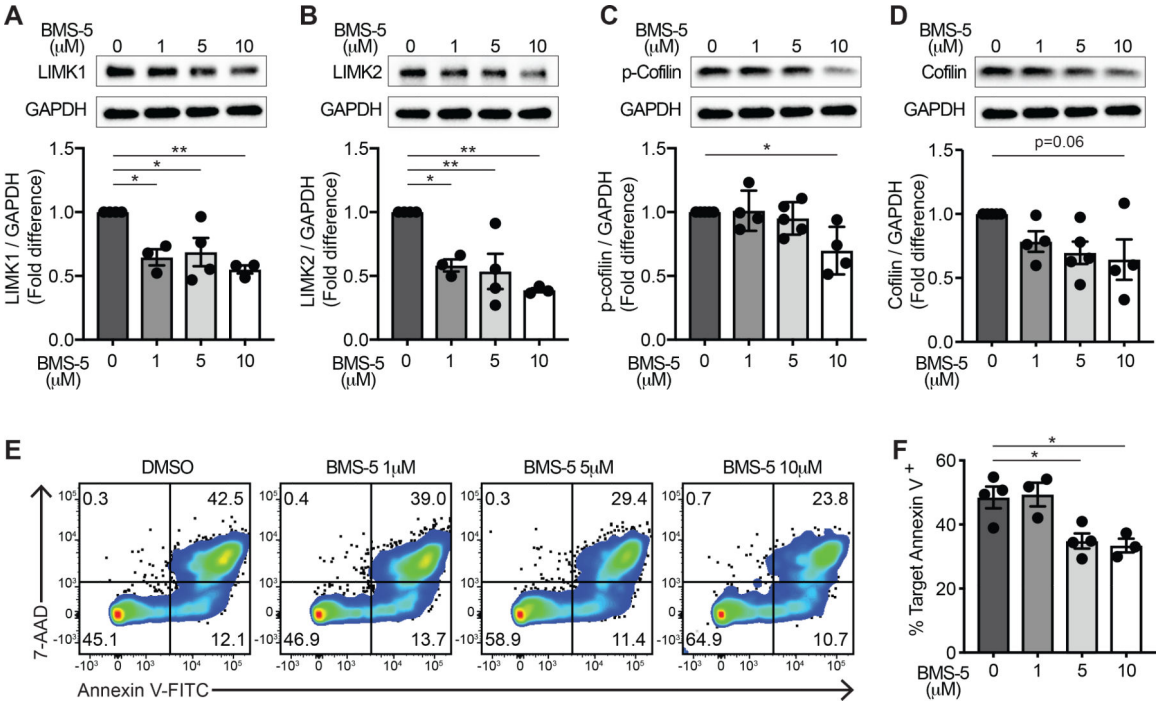

Figure 3. LIMK inhibition impairs NK cell cytotoxicity.

Human primary NK cells were exposed to increasing concentrations of the LIMK inhibitor BMS-5 for 48 hours in culture and protein was extracted. Protein expression was analyzed by Western immunoblotting for each of the indicated proteins and normalized to GAPDH as a loading control. Relative expression of **(A)** LIMK1, **(B)** LIMK2, **(C)** p-cofilin, and **(D)** cofilin was quantified after NK cells were exposed to 1 μM, 5 μM, and 10 μM BMS-5 and fold differences were calculated relative to vehicle control. **(E)** BMS-5-exposed NK cells were co-incubated with K562 target cells for 4 hours and target cell apoptosis was assessed by annexin V and 7-AAD staining as in the representative flow cytometry plots. Quadrant numbers indicate % of target cells. **(F)** Target cell apoptosis was quantified by annexin V staining and compared in LIMK inhibitor-exposed NK cells relative to control conditions for n=3–5 experiments. Bar graphs express mean ± SEM with individual data points. *p<0.05, **p<0.005 by one-way ANOVA with Tukey's multiple comparisons test.

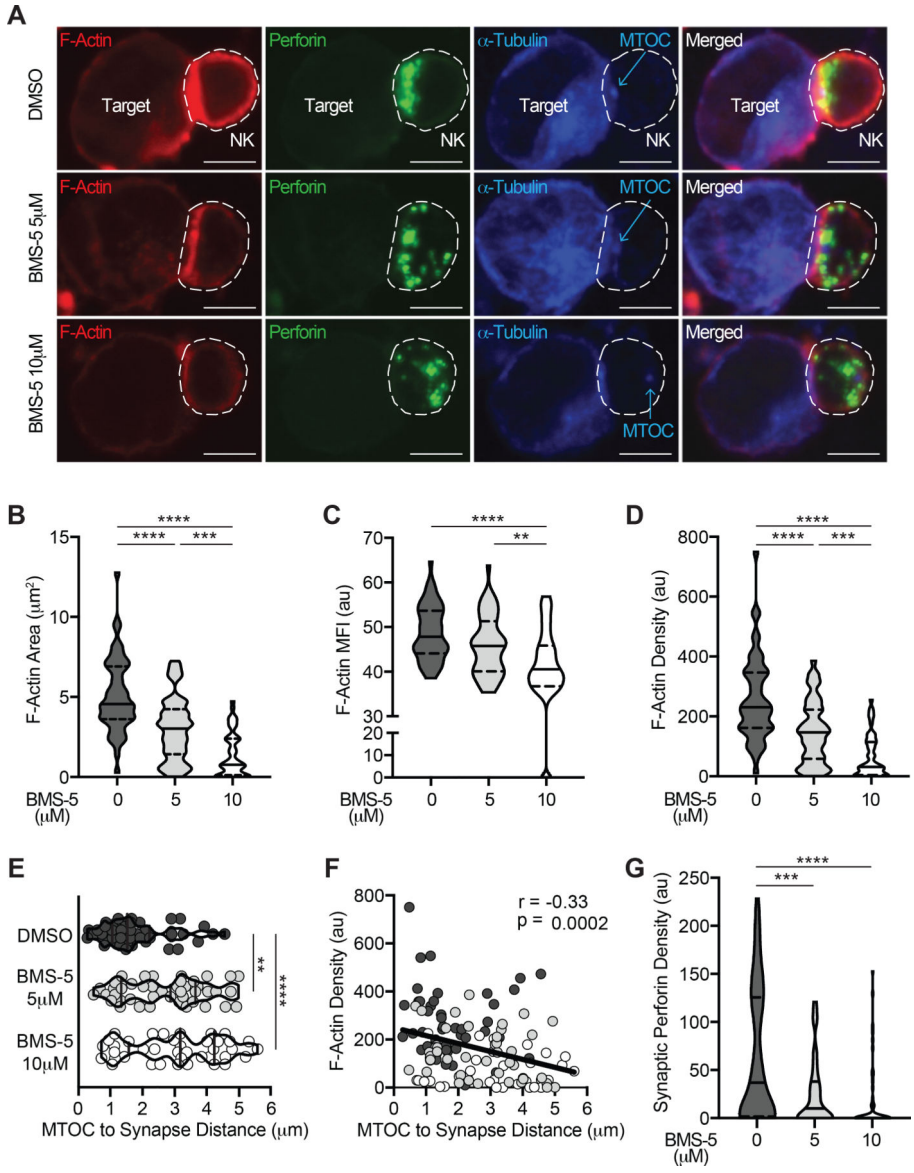

Figure 4. LIMK inhibition disrupts F-actin accumulation and MTOC polarization to the target cell immune synapse.

NK cells were exposed to the LIMK inhibitor BMS-5 for 48 hours prior to co-incubation with K562 target cells for 2 hours. **(A)** Confocal microscopy was utilized to image NK:target conjugates for intracellular F-actin (phalloidin AF555, red), perforin (AF488, green), and α-tubulin (AF647, blue) in control relative to 5 μM and 10 μM BMS-5 conditions. The NK cell is outlined for visualization. Quantitative analysis of F-actin accumulation at the immune synapse was measured by **(B)** area, **(C)** mean fluorescence intensity (MFI), and **(D)** integrated density (area x MFI) at the interface with the target cell. **(E)** The NK cell microtubule organizing center (MTOC) was identified as a discrete α-tubulin signal (as noted in panel A) and the distance from MTOC to the centroid of the immune synapse was calculated for each NK:target conjugate. Violin plots depict density distribution with median (line) and interquartile ranges (dashed line) with individual NK:target conjugate data points

amongst LIMK inhibition conditions (white=10 μM BMS-5; light grey=5 μM BMS-5) relative to DMSO control (dark grey). **(F)** The relationship between F-actin density and MTOC to synapse distance was determined and Pearson correlation coefficient and significance are noted. **(G)** NK cell perforin density (area x MFI) at the synapse was quantified for each NK:target conjugate in n=3 experiments; 15–20 NK:target conjugates imaged per condition per experiment and experiments were pooled for analysis. Scale bar = 5 μm. **p<0.005, ***p<0.0005, ****p<0.0001 by one-way ANOVA with Tukey's multiple comparisons test.

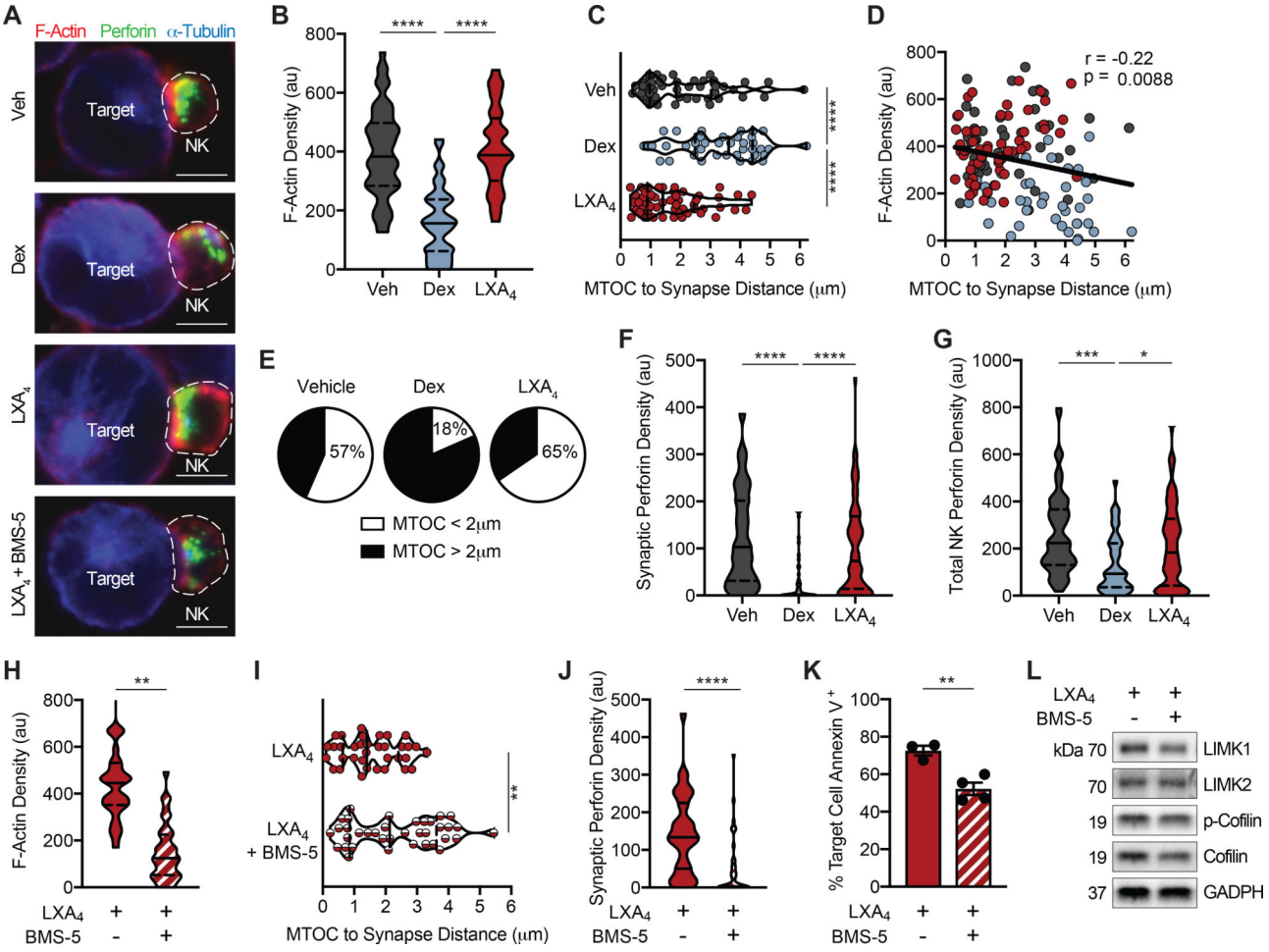

Figure 5. Dexamethasone and LXA_4 differentially regulate NK cell immune synapse and MTOC cytoskeletal rearrangement.

NK cells were exposed to dexamethasone, LXA_4, or vehicle control for 48 hours prior to co-incubation with K562 target cells for 2 hours. In some experiments, NK cells were pre-treated with the LIMK inhibitor BMS-5 (10 μM) prior to exposure to LXA_4. **(A)** Confocal microscopy was utilized to image intracellular F-actin (phalloidin AF555, red), perforin (AF488, green), and α-tubulin (AF647, blue) in NK:target conjugates. **(B)** Immune synapse density of F-actin (area x MFI) was quantified in Veh- (grey), Dex- (blue), or LXA_4-exposed (red) NK cells. **(C)** MTOC to immune synapse distance was calculated for individual NK:target conjugates in each condition. **(D)** The relationship between F-actin density and MTOC to synapse distance was determined and Pearson correlation coefficient and significance are noted. **(E)** Pie charts depict the percentage of NK cells with MTOC < 2 μm from the immune synapse (white) in each condition. The density of NK cell perforin within the immune synapse (**F**) and the entire NK cell (**G**) was calculated. ≥ 45 NK:target conjugates per condition were imaged from 3 individual experiments. NK:target conjugates were analyzed by confocal microscopy for **(H)** F-actin accumulation at the immune synapse, **(I)** MTOC to synapse distance, and **(J)** synaptic perforin content and **(K)** target cell apoptosis by flow cytometry in NK cells exposed to LXA_4 in the presence or absence of the LIMK inhibitor BMS-5. **(L)** Expression of LIMK pathway proteins was assessed by Western

immunoblotting of NK cells exposed to LXA_4 in the presence or absence of the LIMK inhibitor BMS-5. n=2 experiments, ≥ 35 NK:target conjugates were imaged per condition. Violin plots show distribution density with median (line) and quartiles (dashed line). Bars express mean ± SEM. Scale bar = 5 μm. *p<0.05, **p<0.005, ***p<0.0005, ****p<0.0001 by one-way ANOVA with Tukey's multiple comparisons test or two-tailed Student's t-test.